

A tensor-based analysis of orientations in point patterns using the log-Euclidean metric

Bryony Hill*, Elke Thönnnes and Wilfrid Kendall

Department of Statistics, University of Warwick

1 Introduction

Point patterns have been studied extensively (see for example Diggle (1983)) with the major focus being on inter-point distances. However, little work has been done on the directional relationship between points. In this paper we consider point processes arising from some underlying unknown fibre process and how these fibres can be inferred from the point pattern.

2 Applications

Such point patterns arise in a variety of natural environments. The application considered here is of sweat pore patterns on fingerprint ridgelines. The underlying curve structure is the dense set of approximately locally-parallel ridgelines (which form the fingerprint) along which pores are located, usually close to the centre of the ridge (see Figure 1).

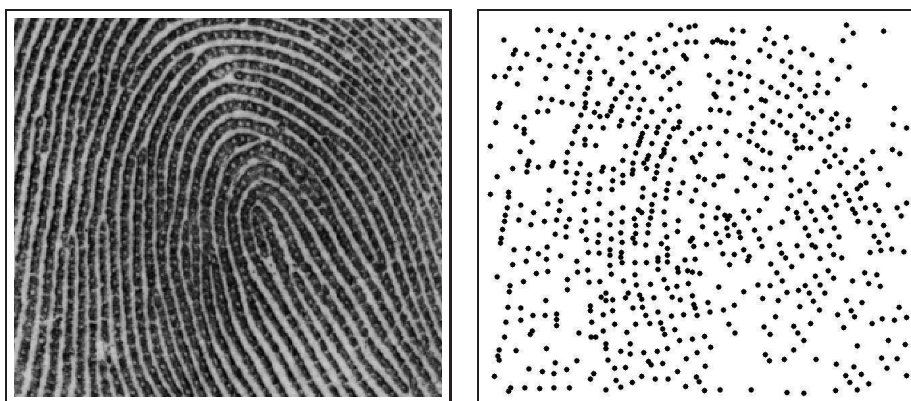


Figure 1: Left: Fingerprint a002-05 from the *NIST Special Database 30*. The sweat pores appear as small light-coloured circles along the ridges. Right: The pore pattern of fingerprint a002-05, identified using computational techniques.

Other applications include the identification of seismic faults from earthquake locations and cenotes (surface connections to underground water bodies) located along the ridge of the Chicxulub crater in the Yucatán Peninsula, Mexico. A 3-dimensional application can be seen in galaxies which tend cluster along *filaments* forming a web-like structure.

3 Point Pattern Analysis

Glancing at the pore pattern in Figure 1, as an example of a point pattern arising from a fibre process, it is easy to perceive the underlying ridge structure. Stevens (1977) hypothesised that when perceiving the structure of patterns such as this, the local parallelism between pairs of nearby points is fundamental, and that the visual system assumes that locally orientations are relatively stable.

The analysis proposed here follows Stevens' supposition by first estimating local orientations within the point pattern using tensors, and then interpolating these estimates to obtain a complete tensor field of orientation estimates. This tensor field can be used along with MCMC methods to sample from the fibre distribution (ridgeline distribution) conditional on the point pattern.

3.1 Su's Mapping and Tensor Method

Su (2009) estimates the local orientation by creating a 2-dimensional tensor (positive-definite symmetric matrix) at each point whose principal eigenvector indicates the most likely direction of the underlying fibre.

The tensor is created at point P by applying a non-linear transformation to all other points Q_i , that preserves the orientation of the line segment (P, Q_i) but transforms its length to

$$w_i = \exp\left(-\frac{\text{dist}(P, Q_i)}{2\sigma^2}\right)$$

where $\text{dist}(P, Q_i)$ is a measure of distance between P and Q_i and σ is a scaling parameter. Hence $Q_i = (\text{dist}(P, Q_i) \cos \theta_i, \text{dist}(P, Q_i) \sin \theta_i)$ is transformed to $\tilde{Q}_i = (w_i \cos \theta_i, w_i \sin \theta_i)$.

A copy of each of the transformed \tilde{Q}_i is rotated by π about the point P and added to the set of transformed points $\{\tilde{Q}_i\}$ to ensure that the mean of all the points is P . This also helps to reduce any boundary effects.

The tensor at P is then calculated by

$$T = \sum_i (w_i \cos \theta_i, w_i \sin \theta_i)^T (w_i \cos \theta_i, w_i \sin \theta_i)$$

where the sum is over both the original and the rotated sets of transformed points.

The tensor's principal eigenvector gives the principal axis along which the variance of the data is maximised. This implies that the $(w_i \cos \theta_i, w_i \sin \theta_i)$ are more dispersed along this axis than any other. Hence if the original untransformed points Q_i were projected onto the principal axis, they would lie relatively close to the initial point P suggesting that the principal axis is a good estimate of the fibre orientation.

3.2 Interpolation and Smoothing

The result of Su's method is a sparse set of tensors each associated with one point in the point pattern. In order to make inferences about the underlying fibre structure it is useful to interpolate these tensor points.

3.2.1 Tensor Metrics

Interpolation of tensors inevitably requires a notion of tensor metric. We briefly discuss a few of the metrics which have been proposed here, for a more extensive account of tensor metrics see Dryden *et al.* (2008).

The standard metric when working with matrices is the *Euclidean* metric where the elements of the matrix are operated on separately. The issue with using this metric with tensors is that tensors are specific matrices with properties that shouldn't be ignored by the metric space. For example, Euclidean extrapolation of two tensors will eventually lead to negative eigenvalues appearing, and Euclidean interpolation can lead to a 'ballooning' effect of the determinant.

An alternative is the *Riemannian* metric proposed in Pennec *et al.* (2006). The affine-invariance properties of this metric make it ideal for working with tensors, however for multilinear interpolation like the Euclidean weighted mean calculations can be computationally expensive. The Fréchet mean (which minimises the least square distances) does not have an explicit solution due to the curvature of the Riemannian manifold. Hence these weighted averages are approximated through a Newton gradient descent method.

Arsigny *et al.* (2006), proposed a solution to the complexity of interpolation - the *Log-Euclidean* metric. The principle of the Log-Euclidean metric is that the logarithm function is a bijective map from the tensor manifold Sym_2^+ to the space of symmetric matrices Sym_2 . So any problem in tensor space can be mapped to Sym_2 , solved in Euclidean space, and converted back, hence the term Log-Euclidean.

The weighted Log-Euclidean Fréchet mean of n tensors T_1, T_2, \dots, T_n with weights w_1, w_2, \dots, w_n is given by

$$\bar{T} = \exp \left\{ \frac{\sum_{i=1}^n w_i \log(T_i)}{\sum_{i=1}^n w_i} \right\} \quad (1)$$

The Log-Euclidean metric doesn't have all the affine-invariant properties of the Riemannian metric, but it is invariant to orthogonal transformations and scaling, making it acceptable as a tensor metric. The actual results of Log-Euclidean interpolation are very similar to those of the affine-invariant Riemannian interpolation and significantly better than the Euclidean interpolation.

3.2.2 Kernel-Based Smoothing and Interpolation

The interpolation method proposed here calculates the tensor S_x at any location x in the space by taking the Log-Euclidean average of *all* tensors T_i at points p_i , and weighting them by a function of the distance between p_i and x .

$$S_x = \exp \left(\frac{\sum_i f(\text{dist}(x, p_i)) \log(T_i)}{\sum_i f(\text{dist}(x, p_i))} \right) \quad (2)$$

By taking into account all tensors the interpolation induces a smoothing effect. If the tensor T_i , calculated at p_i (as outlined in section 3.1), does not give a good estimation of local fibre orientation then the tensors at points around p_i will tend to dominate T_i .

The function f was chosen to be a Gaussian function with mean 0 and with variance parameter h^2 , as it is infinitely smooth and assigns large weights to points within a certain radius of x and thereafter weightings decrease very quickly.

3.3 Results

Figure 2 shows the resultant principal-eigenvector gradient field when this method is applied to the pore pattern in Figure 1. It is evident from this example that this method is effective in interpolating over areas with missing pores. The smoothing effect is beneficial in this application as the ridgelines of fingerprints are locally parallel so all pores within a local area are likely to have the same underlying ridge orientation. However, the interpolated gradient field fails to follow the underlying ridges around the edges where pores are very sparse and also in the central region near the loop of the fingerprint.

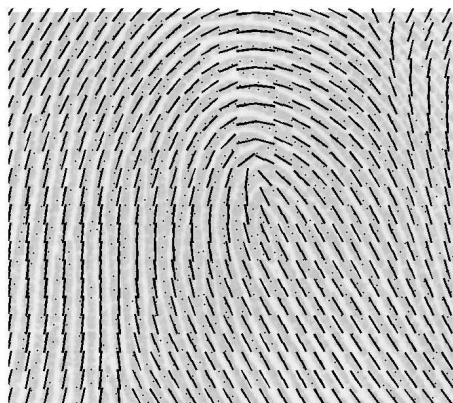


Figure 2: Gradient field of the principal eigenvectors of interpolated tensors, with $h = 30$ (dots represent the pores)

4 Conclusions and Further Work

This method gives us an estimate of a gradient field which is integrated by the fibres that generate the point pattern. Areas for further work include accounting for and correcting the bias caused by areas of high curvature in the fibre process (see, for example, the centre of Figure 2) and estimating the variance of the gradient field calculated using this method.

We are currently experimenting with an MCMC algorithm to estimate the locations of the fibres (and the allocation of points to fibres), which deals with much of the central region problem mentioned above.

References

- Arsigny, V., Fillard, P., Pennec, X. and Ayache, N. (2006). Log- Euclidean Metrics for Fast and Simple Calculus on Diffusion Tensors. *Magnetic Resonance in Medicine*, 56(2):411-421.
- Diggle, P.J. (1983). *Statistical Analysis of Spatial Point Patterns*. 2nd ed.. Academic Press.
- Dryden, I.L., Koloydenko, A. and Zhou, D. (2008). Non-Euclidean statistics for covariance matrices, with applications to diffusion tensor imaging. *Submitted for publication*.
- Pennec, X., Fillard, P. and Ayache, N. (2006). A Riemannian Framework for Tensor Computing. *International Journal of Computer Vision*, 66(1):41-66.

- Stevens, K.A. (1977). Computation of Locally Parallel Structure. *Journal of the Optical Society of America*, 67:1401.
- Su, J. (2009). A Tensor Approach to Fingerprint Analysis. *PhD Thesis, University of Warwick*.
- Su, J., Hill, B., Kendall, W.S. and Thönnies, E. (2008). Inference for point processes with unobserved one-dimensional reference structure. *CRiSM Report No. 08-10*
- Watson, C. NIST Special Database 30: Dual Resolution Images from Paired Fingerprint Cards. *National Institute of Standards and Technology, Gaithersburg*.